http://dx.doi.org/10.7567/JJAP.52.05EA02

Plasma Characteristics of Inductively Coupled Plasma Using Dual-Frequency Antennas

Tae Hyung Kim[1], Kyong Nam Kim[1], Anurag Kumar Mishra[1], Jin Seok Seo[1], Ho Boem Jeong[1], Jung Oun Bae[1], and Geun Young Yeom[1,2]

[1]*Department of Advanced Materials Engineering, Sungkyunkwan University, Suwon, Gyeonggi 440-746, Republic Korea*
[2]*Sungkyun Advanced Institute of Nanotechnology (SAINT), Sungkyunkwan University, Suwon, Gyeonggi 440-746, Republic Korea*

Received November 13, 2012; accepted February 19, 2013; published online May 20, 2013

The plasma characteristics of inductively coupled plasma (ICP) sources operated with dual-frequency antennas with frequencies of 2 and 13.56 MHz were investigated and compared with a source operated with a single-frequency antenna at 13.56 MHz. Improved plasma characteristics such as higher plasma density, lower plasma potential, and lower electron temperature were observed with the dual-frequency ICP source owing to the high absorbed power through the lower driving of the frequency antenna. Also, the variation of the dual-frequency power ratios changed the electron energy distribution. Therefore, when silicon was etched using the dual-frequency ICP with CF_4/Ar, the maximum etching selectivity of silicon over the photoresist could be observed at a 2 MHz rf power ratio of approximately 70% possibly due to the different gas dissociation characteristics for different dual-frequency power ratios, even though the etching rate of silicon increased with the 2 MHz power ratio owing to the increased plasma density. In addition, by using the dual-frequency ICP antennas instead of the single-frequency antenna, the plasma uniformity was also improved.

1. Introduction

Controlling plasma characteristics such as plasma density, plasma potential, electron temperature, and plasma uniformity is the most important factor in developing next-generation plasma equipment for processing various materials. In particular, obtaining uniform plasma over a large-area substrate in addition to high-density plasmas is one of the most important issues for the plasma processing of next-generation semiconductors and flat-panel displays.

Currently, among the various plasma sources, capacitively coupled plasma (CCP) sources and inductively coupled plasma (ICP) sources are being widely investigated and applied for the semiconductor processing.[1–6] CCP sources are used owing to the excellent plasma uniformity over the substrate even though the plasma density is only of $10^{10}/cm^3$ order. On the other hand, ICP sources have a plasma density higher than $10^{11}/cm^3$; therefore, higher-rate processing is possible at a low pressure in addition to easier control of the ion energy to the substrate than for CCP sources. However, owing to the long antenna length, spiral-type ICP sources tend to produce less uniform plasmas over the substrate area than CCP sources and, as the size of the plasma source is increased, the plasma uniformity tends to deteriorate owing to the standing-wave problem.[7–11] In addition, the higher degree of gas dissociation observed for ICP sources due to the high electron temperature causes another problem of low etching selectivity over mask materials during the etching of semiconductor devices.[12–14]

Recently, dual-frequency operation, which uses two rf powers with significantly different frequency on the same electrode, has been intensively investigated for CCP sources.[15–24] For CCP sources, a dual frequency was used to control the ion flux and ion energy to the substrate separately using the higher-frequency rf power and lower-frequency rf power, respectively. In addition, plasma sources operating at different radio frequencies is known to result in different electron energy distribution; therefore, by using two different frequencies instead of a single rf frequency, that is, by using a dual-frequency operation, the plasma characteristics can be varied by varying ratio power ratio of used frequencies. However, a dual-frequency CCP still possesses a lower plasma density than ICP owing to the inherently low ionization rate of CCP. To obtain a higher plasma density, an rf frequency power higher than about 30 MHz can be utilized for dual-frequency CCP as the higher-frequency rf power; however, this can cause a plasma uniformity problem due to the standing-wave effect.

Dual-frequency ICP has also been investigated as a mean of changing the plasma characteristics by adding a second rf power to the ICP source with a different rf frequency; however, the exact comparison between a single-frequency ICP and a dual-frequency ICP was not possible owing to the differences in the total power applied to the ICP source.[25)] In this study, the plasma characteristics of spiral-type ICP sources operated using dual frequencies of 2 and 13.56 MHz were investigated and compared with those operated with a single-frequency of 13.56 MHz while keeping the total rf power the same. The plasma characteristics such as plasma density, plasma potential, and electron temperature were measured with a Langmuir probe, and the plasma uniformity was also compared to investigate the possible application of dual-frequency ICP to large-area wafer processing.

2. Experimental Methods

A schematic diagram of the large-area ICP system used in this experiment is shown in Fig. 1(a). The processing chamber was made of anodized aluminum with an inner diameter of 630 mm and was equipped with a water-cooled substrate holder for large-diameter wafer processing. A 35-mm-thick quartz window was used to cover the top side of the processing chamber. Two different spiral-type ICP antennas were used depending on the mode of operation. For the single-frequency operation, a 15-turn spiral external antenna made of 7 mm Cu tubing was placed on the quartz window. One side of the antenna was connected to a 13.56 MHz rf generator through an L-type matching network, while the other side was directly connected to the ground. When the source was operated in the dual-frequency mode, the spiral antenna was separated into two parts. One was a 12-turn inner antenna operated at 2 MHz, and the other was a 3-turn outer antenna operated at 13.56 MHz. The antenna configuration shown in Fig. 1(a) is for the dual-frequency operation and Fig. 1(b) shows a top view of the

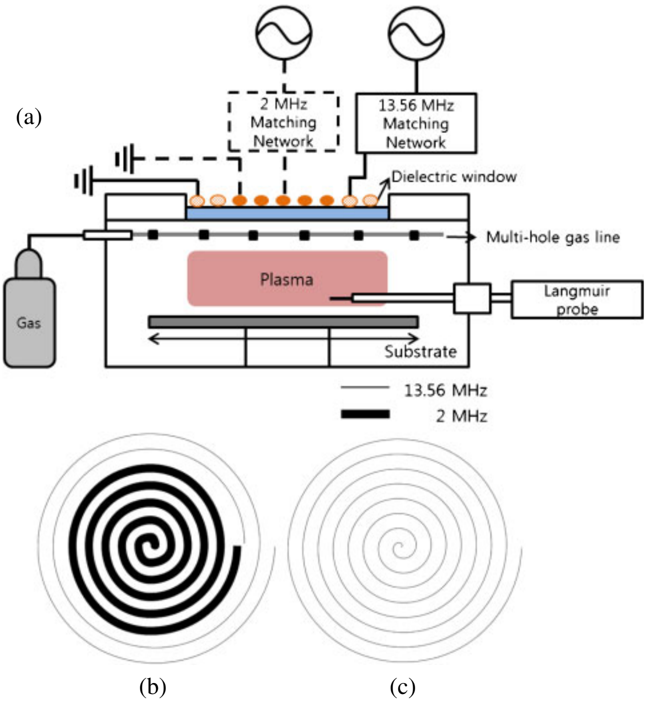

Fig. 1. (Color online) (a) Schematic diagram of ICP system used in this experiment. (b) Dual-frequency ICP source shape using frequency of 13.56 and 2 MHz. (c) Single-frequency ICP source shape using frequency of 13.56 MHz.

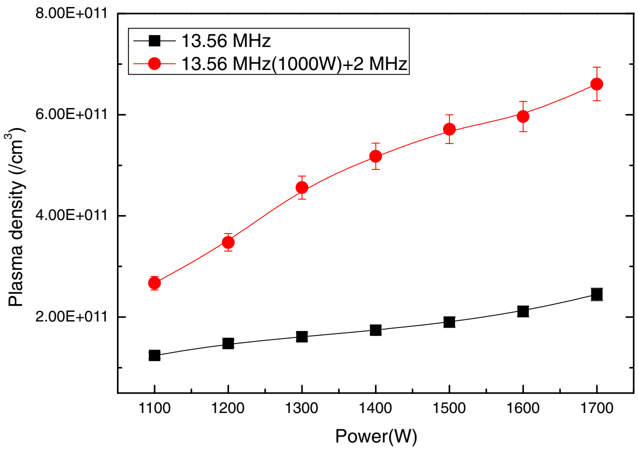

Fig. 2. (Color online) Plasma density of dual-frequency ICP source and single-frequency ICP source as a function of total power. For the dual-frequency mode, the 13.56 MHz rf power was kept at 1000 W and the 2 MHz rf power was varied from 100 to 800 W with 10 mTorr Ar.

spiral-type ICP antenna used for the dual frequency operation in this study. Figure 1(c) shows a top view of the conventional 15-turn spiral-type ICP antenna connected to a 13.56 MHz rf power source for the single-frequency operation.

To investigate the characteristics of the plasmas, a Langmuir probe (Hiden Analytical, ESPION) was installed 3.5 cm below the antenna and at the center of the chamber. The probe was a cylindrical tungsten wire of 0.15 mm diameter and 10 mm length. The probe tip was supported by a ceramic tube, which was 1.2 mm in diameter and enclosed by a compensated electrode. Other plasma parameters such as plasma density (N_i), plasma potential (V_p), and electron temperature (T_e) were obtained using the Langmuir probe. Ion saturation current was measured using the Langmuir probe along the horizontal centerline of the chamber as a measure of plasma uniformity. To correlate the plasma characteristics of the dual-frequency ICP with the material-processing characteristics, photoresist and silicon were etched at a total rf power of 1000 W with 20 mTorr Ar/CF_4 (1 : 10). While etching the samples with the dual-frequency mode, the substrate was biased at -100 or -200 V with a separate 12.56 MHz (not 13.56 MHz) rf power.

3. Results and Discussion

Figure 2 shows the plasma density measured as a function of rf power for both the single frequency of 13.56 MHz and the dual frequencies of 13.56/2 MHz using a Langmuir probe. Ar at a pressure of 10 mTorr was used as the discharge condition. For the dual-frequency operation, 2 MHz rf power was added to the 12-turn inner ICP antenna while a 13.56 MHz rf power of 1000 W was applied to the 3-turn outer ICP antenna. As shown in the figure, with increasing total power, the plasma density increased almost linearly for both the single-frequency operation at 13.56 MHz and the dual-frequency operation at 13.56 MHz (1000 W) + 2 MHz. However, as shown in the figure, the dual-frequency operation showed significantly higher plasma density at the same total rf power. For example, at a total rf power of 1.7 kW, the plasma density measured with the dual-frequency rf power was close to $7 \times 10^{11}/\text{cm}^3$ which is about three times higher than that measured with the single-frequency rf power of 13.56 MHz. In fact, the operation of a spiral-type ICP source at a lower frequency is known to increase the power absorption compared with that operated at a higher frequency because the power absorbed by the electrons in the plasma can be represented in terms of the electric field amplitude E as follows:

$$P_{\text{ohmic}} = \frac{1}{2}|\bar{E}|^2\sigma_{\text{dc}}\frac{\upsilon_{\text{m}}}{\omega^2 + \upsilon_{\text{m}}^2}$$

Where P_{ohmic} is the power absorbed by ohmic heating, σ_{dc} is the DC plasma conductivity, υ_{m} is the collision frequency, and ω is the driving frequency. Also, the electric field E can be represented as $E = J_{\text{T}}^{-}/(\sigma_{\text{p}} + j\omega\varepsilon_0)$ (where J_{T} is the total current, σ_{p} is the plasma conductivity, and ε_0 is vacuum permittivity). As shown, P_{ohmic} is proportional to $|\bar{E}|^2$ and E is inversely proportional to ω. As a result, the operation at 2 MHz produces a higher electric field than that at 13.56 MHz.[26] Therefore, the higher plasma density for the dual-frequency operation is believed to be from the higher power absorption at the lower rf frequency. As shown in Fig. 2(a), a total power of 1000 W operated at 13.56 MHz, the plasma densities for dual-frequency operation and single-frequency operation are different owing to the different configurations of the antenna, shown in Figs. 1(b) and 1(c) for the dual-frequency operation and the single-frequency operation, respectively.

The plasma potentials measured as a function of rf power for both the single 13.56 MHz frequency and the dual frequency of 13.56 MHz (1000 W) + 2 MHz using the Langmuir probe are shown in Fig. 3(a). As shown in

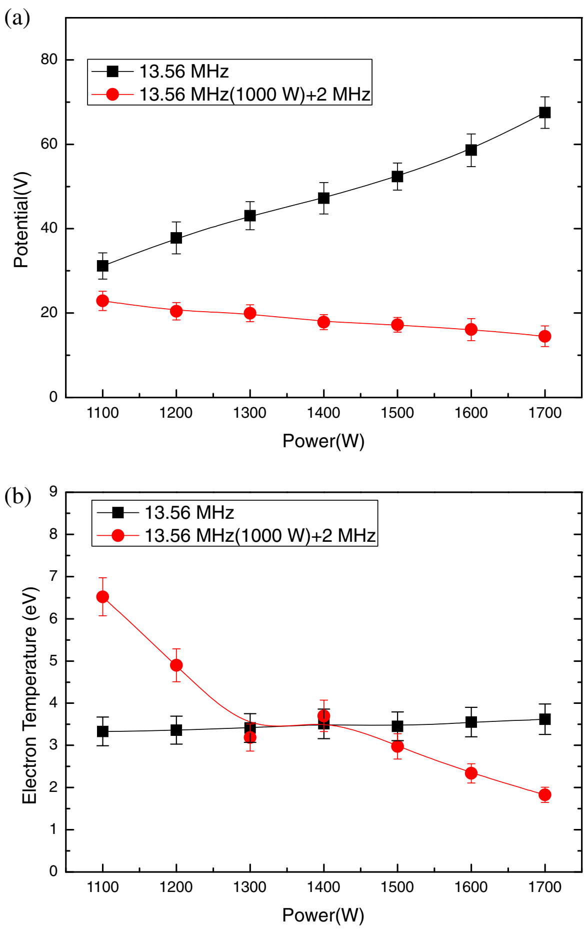

Fig. 3. (Color online) (a) Plasma potential and (b) electron temperature of dual-frequency ICP source and single-frequency ICP source with 10 mTorr Ar.

Fig. 3(a), increasing the single-frequency rf power at 13.56 MHz from 1100 to 1700 W increased the plasma potential almost linearly from about 30 to 68 V. However, in the dual-frequency operation, when 2 MHz rf power was added to the plasma formed at a 13.56 MHz rf power of 1000 W, an increase in the 2 MHz rf power from 100 to 700 W decreased the plasma potential from about 23 to 14 V; therefore, the addition of 2 MHz rf power to the ICP formed by the 13.56 MHz rf power decreased the plasma potential while increasing the plasma density significantly. An increase in the rf power of the plasma source tends to increase the plasma potential owing to the increase in the rf voltage induced on the electrode. Therefore, the increase in plasma potential with the increase in the 13.56 MHz rf power for the single-frequency operation is related to the increase in rf voltage on the ICP source electrode, and therefore to the increased sheath voltage near the ICP source. However, when the ICP source is operated with the dual frequency, because of the decrease in plasma impedance caused by the increase in plasma density when 2 MHz rf power is applied to the inner ICP antenna, the rf voltage on the outer ICP antenna operated at 13.56 MHz is decreased with increasing of 2 MHz rf power, which results in the decrease in the plasma potential. (The rf voltage to the inner antenna operated at 2 MHz is much smaller than that to the outer ICP antenna operated at 13.56 MHz owing to the lower impedance.) Therefore, the decrease in plasma potential is related to the decreased plasma impedance by the addition of 2 MHz rf power.

The electron temperatures measured for the conditions in Fig. 3(a) are shown in Fig. 3(b). When the ICP source was operated with the single 13.56 MHz rf power, the electron temperature increased continuously even though the amount of the increase was not significantly high. However, for the dual-frequency operation, even though the electron temperature was initially higher than that for the single-frequency operation at low total rf powers of 1100–1400 W, possibly due to the different antenna configurations as shown in Figs. 1(b) and 1(c), the increase in total rf power upon the addition of 2 MHz rf power to the rf power of 1000 W at 13.56 MHz decreased the electron temperature monotonically. Eventually, when a total rf power of 1.7 kW was applied to the plasma, the dual-frequency operation (700 W rf power at 2 MHz + 1000 W at 13.56 MHz) showed an electron temperature of about 2 eV, which is about 1.6 eV lower than that for the single-frequency operation (1700 W at 13.56 MHz) of about 3.6 eV. A previous study by Godyak et al.[27)] showed that, at high plasma density, the increased electron–electron collisions (because $v_{ee} \propto n\varepsilon^{3/2}$, where v_{ee} is the electron–electron collision frequency, n is the plasma density, and ε is the energy of electron) maxwellianize the low-energy part of the electron energy distribution. Also, a two-step ionization processes via atomic excited states mainly controls the ionization, which leads to the reduction of the electron temperature with increasing plasma density. In our experiment, as shown in Fig. 2, the plasma density significantly increased with the addition of the 2 MHz power; therefore, the increased plasma density upon adding the 2 MHz power appeared to be related to the decrease in electron temperature.

The higher electron temperature and higher potential of the plasma can increase not only the electrical damage but also the physical damage to the substrate, especially for electronic devices which require plasma processing during the device processing. Therefore, the operation of the ICP source with the dual frequencies of 2/13.56 Hz instead of the single frequency of 13.56 MHz is believed to decrease the possible damage to the sample during the plasma processing.[28–31)]

In large-scale substrate processing, one of the most important parameters is the plasma uniformity over the substrate surface. In this study, the plasma uniformity was also measured for the dual frequency operation using the Langmuir probe and the uniformity was compared with that for a single frequency of 13.56 MHz. Figure 4(a) shows the ion saturation current measured as a function of the radial position of the chamber for the single-frequency operation at 1.1 kW and 13.56 MHz and for the dual-frequency operation of 800 W at 13.56 MHz + 300 W at 2 MHz. Ar at a pressure of 10 mTorr was used and the ion density was measured by scanning the Langmuir probe from the center to the edge of the chamber while the plasma was turned on. The measured ion density was normalized to the ion current density at the center. As shown, the ion current density was maximum near the center of the chamber and decreased slowly when the probe was moved away from the toward the chamber wall for both the single-frequency operation and the

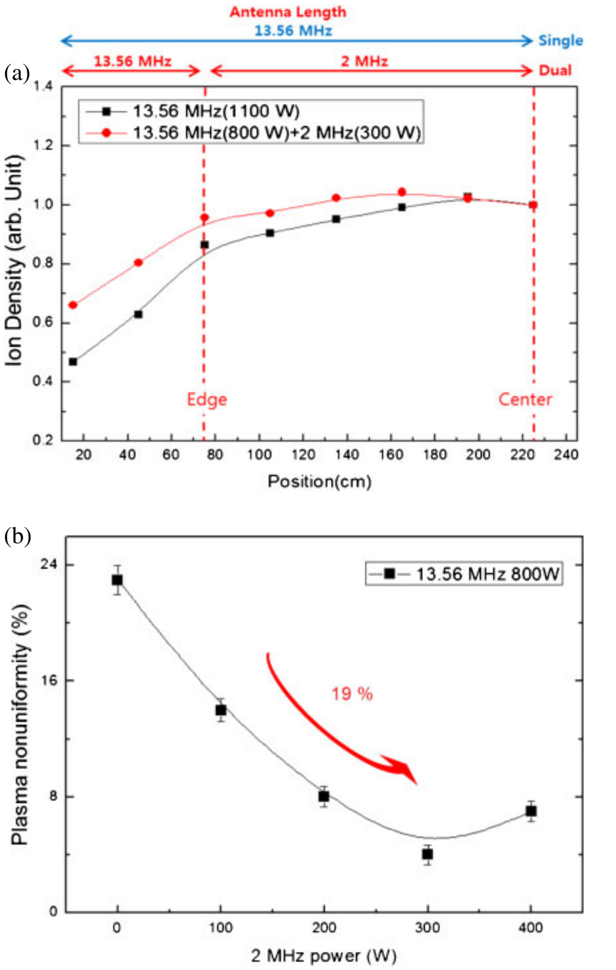

Fig. 4. (Color online) (a) Ion density measured with a Langmuir probe along the chamber centerline for the single-frequency source power (13.56 MHz, 1100 W) and the dual-frequency source power (13.56 MHz, 800 W and 2 MHz 300 W) with 10 mTorr Ar. (b) Plasma nonuniformity of the dual-frequency ICP source measured with the Langmuir probe as a function of 2 MHz rf power from 0 to 400 W in addition to 800 W at rf power 13.56 MHz.

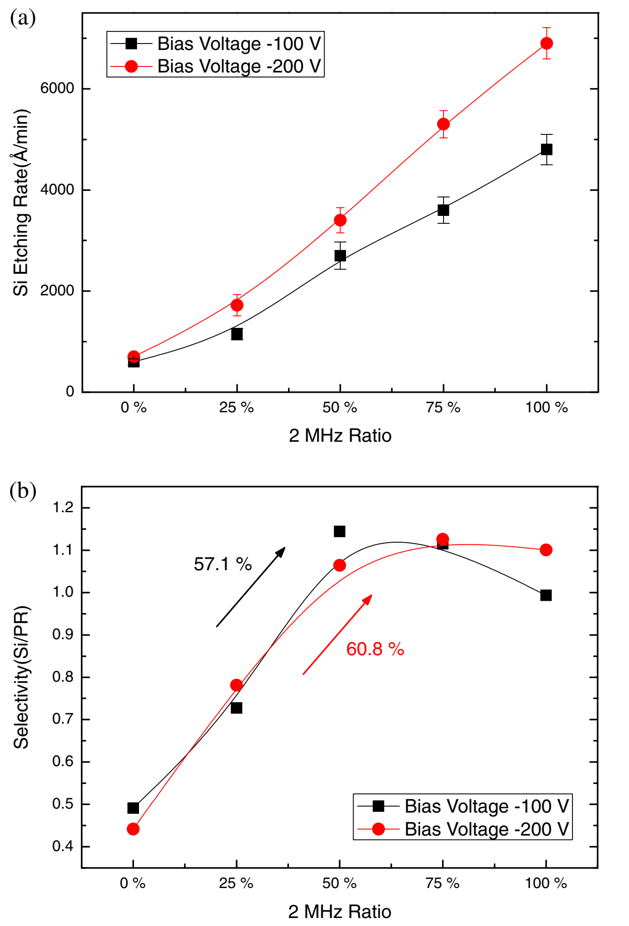

Fig. 5. (Color online) (a) Silicon etching rate and (b) etching selectivity of silicon over photoresist measured as a function of ratio of 13.56 and 2 MHz rf powers while maintaining the total rf power at 1000 W. The rf frequency for substrate biasing was 12.56 MHz (−100 and −200 V) and a 20 mTorr CF_4/Ar (10 : 1) gas mixture was used.

dual-frequency operation. However, compared with the single-frequency operation, the dual-frequency operation produced better plasma uniformity. For example, the plasma nonuniformity with in the diameter of the 2 MHz antenna (300 mm diameter), was 8% for the single-frequency operation and about 4% for the dual-frequency operation.

In fact, the 2 MHz rf power acted as a separate mean of controlling the plasma uniformity in the dual-frequency operation that was unavailable in the single-frequency operation of the ICP source. Figure 4(b) shows the plasma nonuniformity measured as a function of 2 MHz rf power for the dual-frequency operation of 800 W at 13.56 MHz + 2 MHz with 10 mTorr Ar. As shown, as the 2 MHz rf power was increased from 0 to 300 W, the plasma nonuniformity decreased significantly from about 24 to 4% owing to the increased plasma density at the center of the chamber. However, when the 2 MHz rf power was increased further to 400 W, the plasma nonuniformity increased to 7% owing to the excessive plasma density at the center of the chamber induced by the 2 MHz rf power. Therefore, there was an optimum combination of the powers at the two frequencies for maximum plasma uniformity. It is believed that, by extending the concept of the dual-frequency rf power source to a larger scale, better plasma uniformity that can be applicable to a 450 mm-diameter-wafer system can be obtained. In fact, if the two separate coils of the dual-frequency source are operated with the same rf frequency, it is expected that a similar effect can be obtained by splitting the rf power between the two coils. Therefore, the improved plasma uniformity obtained by the dual-frequency rf power source in this experiment is more related to the power-splitting effect than to the use of dual-frequencies.

To correlate the plasma characteristics of the dual-frequency-generated ICP to material processing, silicon was etched by varying the ratio of the 2 and 13.56 MHz rf powers for two different rf substrate biases of −100 and −200 V with a separate 12.56 MHz rf power supply. The effect of the rf power ratio on the etching rate of silicon and the etching selectivity over a photoresist are shown in Figs. 5(a) and 5(b), respectively. The total rf power (2 MHz + 13.56 MHz) was maintained at 1000 W and 20 mTorr Ar/CF_4 (1 : 10) was used as the etching gas mixture. As shown in the figure, increasing the 2 MHz rf power while maintaining the total rf power increased the silicon etching rate almost linearly with increasing ratio of the 2 MHz rf power. The etching selectivity of silicon over the photoresist were also increased with increasing ratio of 2 MHz rf power up to a value of 70% and further increases in the 2 MHz rf power ratio appeared to decrease the etching selectivity. The increase in the etching rate of silicon with increasing 2 MHz power ratio is related to the increased plasma density as shown in Fig. 2. However, as the ratio between the 2 and 13.56 MHz rf powers is varied, the electron energy distribution is varied, which changes the gas dissociation characteristics in addition to the plasma density. A separate study on the electron energy distribution for a dual-frequency system showed that increasing the 2 MHz rf power while maintaining the 13.56 MHz rf power increased the density of high-energy electrons, whereas increasing the 13.56 MHz rf power while maintaining the 2 MHz rf power increased the density of low-energy electrons.[32] Thus, an increase in the 2 MHz power ratio initially increases the etching rate of silicon owing to the increased dissociation of CF_4 gas. However, when the 2 MHz power ratio is higher than 70%, the fluorocarbon polymer deposition on the photoresist is decreased owing to the lack of CF_2 due to excessive CF_4 dissociation. Therefore, the maximum silicon etching selectivity over the photoresist, shown to be at a 2 MHz rf power ratio of approximately 70%, is believed to be related to the excessive CF_4 gas dissociation caused by varying the electron energy distribution for different ratios between the 2 and 13.56 MHz rf powers. Consequently, it is believed that, by using the dual-frequency ICP source instead of a single-frequency ICP source, not only superior plasma characteristics such as increased plasma density, lower plasma potential, lower electron temperature, and more uniform plasma but also the ability to vary the gas dissociation characteristics can be realized.

4. Conclusions

In this study, the plasma characteristics of conventional spiral-type ICP sources operated using dual-frequency antennas with frequencies of 2 and 13.56 MHz were compared with those operated with a single-frequency antenna at 13.56 MHz. The dual-frequency operation of the ICP source showed higher plasma densities than the single 13.56 MHz rf power operation at the same total rf power owing to the higher power absorption at 2 MHz than at 13.56 MHz. Also, compared with the 13.56 MHz single-frequency operation, the spiral-type ICP source operated with the dual frequency showed a lower plasma potential and a lower electron temperature, especially at a high 2 MHz rf power ratio. The lower plasma potential and lower electron temperature can decrease the electrical damage and physical damage to the substrate during the plasma operation; therefore, the dual-frequency operation of the ICP source can be beneficial during plasma processing compared with the single-frequency operation at 13.56 MHz. In addition, when the plasma uniformity was measured, by controlling the ratio of the powers of the dual frequencies, better plasma uniformity could be obtained than that for the single-frequency operation, in addition to a higher plasma density, lower electron temperature, and lower plasma potential. Therefore, it is believed that the operation of a spiral-type ICP source using dual frequencies of 2 and 13.56 MHz is applicable to next-generation large-area wafer processing.

Acknowledgments

This work was supported by an Industrial Strategic Technology Development Program [10041926 (Development of High Density Plasma Technologies for Thin Film Deposition of Nanoscale Semiconductor and Flexible Display Processing)] funded by the Ministry of Knowledge Economy (MKE, Korea). This work was also supported in part by the World Class University Program of the National Research Foundation of Korea (Grant No. R32-2008-000-10124-0).

1) D. M. Manos and D. L. Flamm: *Plasma Etching: An Introduction* (Academic Press, New York, 1989).
2) J. Hopwood: Plasma Sources Sci. Technol. **1** (1992) 109.
3) J. P. Holland, B. R. Richardson, E. Bogle, W. Li, Y. Melaku, H. T. Nguyen, E. A. Peltzer, and D. C. Gates: Proc. SPIE **1803** (1993) 258.
4) M. S. Barnes, J. C. Forster, and J. H. Keller: Appl. Phys. Lett. **62** (1993) 2622.
5) J. H. Keller, J. C. Forster, and M. S. Barnes: J. Vac. Sci. Technol. A **11** (1993) 2487.
6) Y. Yang and M. J. Kushner: J. Appl. Phys. **108** (2010) 113306.
7) A. J. Lamm: J. Vac. Sci. Technol. A **15** (1997) 2615.
8) R. L. Kinder and M. J. Kushner: J. Vac. Sci. Technol. A **19** (2001) 76.
9) P. Chabert, J.-L. Raimbault, J.-M. Rax, and A. Perret: Phys. Plasmas **11** (2004) 4081.
10) Y. Wu and M. A. Lieberman: Plasma Sources Sci. Technol. **9** (2000) 210.
11) T. Meziani, P. Colpo, and F. Rossi: Plasma Sources Sci. Technol. **10** (2001) 276.
12) K. Kato, J. Emi, and S. Iizuka: J. Plasma Fusion Res. SERIES **8** (2009) 1287.
13) M. Dhayal, D. Forder, R. D. Short, and J. W. Bradley: Vacuum **70** (2003) 67.
14) N. Sato, S. Iizuka, T. Koizumi, and T. Takada: Appl. Phys. Lett. **62** (1993) 567.
15) T. Kitajima, Y. Takeo, Z. L. Petrovic, and T. Makabe: Appl. Phys. Lett. **77** (2000) 489.
16) S. Rauf and M. J. Kushner: IEEE Trans. Plasma Sci. **27** (1999) 1329.
17) P. C. Boyle, A. R. Ellingboe, and M. M. Turner: J. Phys. D **37** (2004) 697.
18) H. C. Kim and J. K. Lee: Phys. Rev. Lett. **93** (2004) 085003.
19) J. K. Lee, O. V. Manuilenko, N. Yu. Babaeva, H. C. Kim, and J. W. Shon: Plasma Sources Sci. Technol. **14** (2005) 89.
20) Q. H. Yuan, G. Q. Yin, Y. Xin, and Z. Y. Ning: Phys. Plasmas **18** (2011) 053501.
21) D. H. Kim, S. H. Cho, N. E. Lee, and K. C. Kwon: Jpn. J. Appl. Phys. **44** (2005) 5856.
22) D. H. Kim, C.-M. Ryu, S. H. Lee, and J. K. Lee: Jpn. J. Appl. Phys. **47** (2008) 7005.
23) C. Ye, Y. Xu, X. Huang, and Z. Ning: Thin Solid Films **518** (2010) 3223.
24) Z.-H. Bi, Z.-L. Dai, X. Xu, Z.-C. Li, and Y.-N. Wang: Phys. Plasmas **16** (2009) 043510.
25) A. Mishra, K. N. Kim, T. H. Kim, and G. Y. Yeom: Plasma Sources Sci. Technol. **21** (2012) 035018.
26) K. N. Kim, J. H. Lim, G. Y. Yeom, S. H. Lee, and J. K. Lee: Appl. Phys. Lett. **89** (2006) 251501.
27) V. A. Godyak, R. B. Piejak, and B. M. Alexandrovich: Plasma Sources Sci. Technol. **11** (2002) 525.
28) S. Siu, R. Patrick, V. Vahedi, S. Alba, G. Valentini, and P. Colombo: Proc. 4th Int. Symp. Plasma Process-Induced Damage, 1999, p. 25.
29) G. S. Hwang and K. P. Giapis: Appl. Phys. Lett. **74** (1999) 932.
30) T. Goto, T. Matsuoka, and T. Ohmi: J. Vac. Sci. Technol. A **27** (2009) 653.
31) X. Li, H. Zhou, R. J. W. Hill, M. Holland, and I. G. Thayne: Jpn. J. Appl. Phys. **51** (2012) 01AB01.
32) A. Mishra, T. H. Kim, K. N. Kim, and G. Y. Yeom: to be published in Plasma Sources Sci. Technol.